Research Article

Rapid Communications in Mass Spectrometry

Received: 9 December 2012 Revised: 2 January 2013 Accepted: 3 January 2013 Published online in Wiley Online Library

Rapid Commun. Mass Spectrom. **2013**, *27*, 805–815
(wileyonlinelibrary.com) DOI: 10.1002/rcm.6503

Rapid differentiation of isomeric lipids by photodissociation mass spectrometry of fatty acid derivatives

Huong T. Pham[1], Adam J. Trevitt[1], Todd W. Mitchell[2] and Stephen J. Blanksby[1]*

[1]ARC Centre of Excellence for Free Radical Chemistry and Biotechnology, School of Chemistry, University of Wollongong, NSW 2522, Australia
[2]School of Health Sciences, University of Wollongong, Wollongong, NSW 2522, Australia

RATIONALE: Both traditional electron ionization and electrospray ionization tandem mass spectrometry have demonstrated limitations in the unambiguous identification of fatty acids. In the former case, high electron energies lead to extensive dissociation of the radical cations from which little specific structural information can be obtained. In the latter, conventional collision-induced dissociation (CID) of even-electron ions provides little intra-chain fragmentation and thus few structural diagnostics. New approaches that harness the desirable features of both methods, namely radical-driven dissociation with discrete energy deposition, are thus required.
METHODS: Herein we describe the derivatization of a structurally diverse suite of fatty acids as 4-iodobenzyl esters (FAIBE). Electrospray ionization of these derivatives in the presence of sodium acetate yields abundant $[M + Na]^+$ ions that can be mass-selected and subjected to laser irradiation ($\lambda = 266$ nm) on a modified linear ion-trap mass spectrometer.
RESULTS: Photodissociation (PD) of the FAIBE derivatives yields abundant radical cations by loss of atomic iodine and in several cases selective dissociation of activated carbon–carbon bonds (e.g., at allylic positions) are also observed. Subsequent CID of the $[M + Na - I]^{\bullet +}$ radical cations yields radical-directed dissociation (RDD) mass spectra that reveal extensive carbon–carbon bond dissociation without scrambling of molecular information.
CONCLUSIONS: Both PD and RDD spectra obtained from derivatized fatty acids provide a wealth of structural information including the position(s) of unsaturation, chain-branching and hydroxylation. The structural information obtained by this approach, in particular the ability to rapidly differentiate isomeric lipids, represents a useful addition to the lipidomics tool box. Copyright © 2013 John Wiley & Sons, Ltd.

Traditional mass spectrometric analysis of fatty acids (FAs) involves: (i) a chemical derivatization step to enhance the volatilization of these lipids; (ii) separation by gas chromatography (GC); and (iii) ionization, most commonly by electron ionization (EI). By far the most widely used method of chemical modification is to convert the free FAs into fatty acid methyl esters (FAMEs), which have desirable chromatographic properties.[1,2] Observation of the molecular ion in a conventional EI (70 eV) spectrum of a FAME allows the assignment of carbon-chain length and degree of unsaturation, complementing information derived from its GC retention time. Unfortunately, the molecular ions arising from EI of FAMEs are typically low in abundance with much of the signal intensity found in peaks corresponding to dissociation and/or rearrangements of the molecular framework, e.g., a base peak at m/z 74 is common and arises from the McLafferty rearrangement.[1,3] Furthermore, even when the stoichiometry of the lipid can be determined from the EI mass spectrum, distinguishing it from possible isomeric variants is difficult due to scrambling of molecular information driven by the high energy of the EI process. For example, EI cannot distinguish unsaturated FAME isomers due to the migration of double bonds prior to dissociation of the molecular ion.[3] Although such effects can be modulated in some instances by reducing the EI energy,[4] in general distinguishing between isomeric FAMEs relies on their separation by GC and comparison of retention times with those of authentic compounds. This too presents challenges where appropriate reference compounds are not available or chromatographic resolution is poor resulting in overlapping peaks.[5,6] The inability to assign fatty acid structures unambiguously or even the possibility of misassignments is thus a significant limitation of current technologies. In particular, such limitations mask the full extent of natural variation in lipid structure (e.g., the positions of branched motifs or site(s) of unsaturation) and thus, the distinct biochemical and biophysical roles of individual lipid species are more difficult to uncover.[7–9]

As a result of these aforementioned limitations in EI analysis of FAMEs, other derivatization strategies have emerged to enhance the structure-specificity of fatty acid analysis by GC/MS. Notable among these are the use of picolinyl esters[10] and 4,4-dimethyloxazoline (DMOX) derivatives.[11,12] These modifications introduce a nitrogen heterocycle that, when subjected to conventional EI, can effectively sequester the

* *Correspondence to:* S. J. Blanksby, ARC Centre of Excellence for Free Radical Chemistry and Biotechnology, School of Chemistry, University of Wollongong, NSW 2522, Australia. E-mail: blanksby@uow.edu.au

charge thus enhancing the abundance of the molecular ion and facilitating the formation of more structurally diagnostic product ions. For example, the observation of a 12 Th (or in some cases 26 Th) peak spacing in EI spectra of picolinyl ester or DMOX derivatives can be used to assign carbon–carbon double-bond position(s) in unsaturated fatty acids.[13] Although this represents a significant improvement over FAME derivatives, there are still limitations in this approach. For example, EI of DMOX derivatives does not yield diagnostic details of methyl branching points within saturated acyl chains.[1,11] Branched lipids, especially methyl branched fatty acids, are widespread in nature[14] where they are thought to have essential roles in metabolism.[15,16] Thus, mass spectrometric methods capable of also revealing lipid isomerism arising from chain-branching are desirable. One approach, pioneered by Zirrolli and Murphy,[17] involved mass-selection of the low-abundance molecular ions arising from EI of FAMEs and subjecting these to low-energy collision-induced dissociation (CID) on a tandem mass spectrometer (MS/MS). The resulting EI-CID mass spectra successfully differentiated non-branched and branched acyl chains. In the case of the straight-chain variants, almost identical product ion abundances arising from the cleavage of every carbon–carbon bond were observed in the EI-CID spectrum and resulted in regular peak spacing of 14 Th. In contrast, for the branched-chain species, carbon–carbon bond cleavage was enhanced on either side of the tertiary carbons leading to a characteristic gap of 28 Th that allowed the position(s) of methyl substitution to be assigned. The mechanism of EI-CID fragmentation was studied by isotope-labelling experiments, which revealed that radical-driven fragmentation was probably responsible for these spectral patterns.[17] Recently, EI-CID was extended by Brenna and co-workers[18] to examine a series of saturated branched-chain FAME synthetic standards. They were able to establish an exhaustive look-up table of diagnostic product ions for determining the methyl branching points. It was noted, however, that the sensitivity in detecting these features reduces as the position of methyl substitution approached the ester moiety. Notably therefore, the predicted peak assigning a branch point at the C3 position is often absent in the EI-CID spectrum. Although powerful, one disadvantage of EI-CID is the inherently low abundance of the required molecular ions such that only a very small number of ionized molecules retain the necessary structural information for MS/MS analysis.

Due to recent advances in fast and efficient liquid chromatography (LC) protocols, LC/MS is gaining wider acceptance as an alternative approach to the identification and quantification of fatty acids in biological extracts.[19,20] The location of double bonds within a particular acyl chain is found to significantly affect the LC separation, providing desirable chromatographic resolution of isomers – particularly in the presence of silver ions[21,22]; however, the unambiguous assignment of this structural feature still relies on retention times and comparison with standard compounds (cf. GC discussion above). Therefore, ion activation methods that produce diagnostic mass spectra and are also compatible with LC protocols are of increasing interest. Given the presence of the carboxylate moiety, $[M-H]^-$ ions generated by electrospray ionization (ESI) are common targets for fatty acid identification in LC/MS protocols. Conventional (low-energy) CID mass spectra of these ions are typically dominated by loss of carbon dioxide and thus do not reveal details of the structure of the hydrocarbon chain although recent work suggests that the relative abundance of these ions can be a useful probe.[23] Hsu and Turk[24] have shown that the addition of lithium salts can give rise to abundant $[M-H+Li_2]^+$ ions that upon CID undergo carbon–carbon bond cleavage at vinylic and allylic positions that can be exploited in localizing double-bond positions. This, and related approaches, have been successfully deployed for the LC/MS identification of unusual fatty acids in complex mixtures.[25] An alternative approach to promote even-electron fragmentation at carbon–carbon double bonds is to undertake chemical modification of the motif itself. For example, ozonolysis of lipids in a thin film[26] or pre-treatment of extracts with osmium tetroxide (OsO_4)[27] modify the targeted functional group by oxidation making it susceptible to cleavage upon CID. Such chemical derivatizations do increase the complexity of the mixture and may cause significant and undesirable changes in LC behaviors depending on how many sites are modified. Alternative methods exploit selective chemistries in the gas phase, such as ozone-induced dissociation[28] and covalent adduct chemical ionization.[2] These are powerful methods for the identification of carbon–carbon double-bond positions in unsaturated lipids and both are compatible with LC/MS workflows but are unable to provide information on other structural features in the lipid such as position(s) of chain branching.

Conceptually, it is attractive to exploit radical-driven dissociation (cf. EI-CID) but in combination with high ion yields, well-defined dissociation energetics and in a manner compatible with LC/MS. In this vein we have recently introduced radical-directed dissociation (RDD) to the structural analysis of complex lipids.[29] In this approach even-electron complexes are formed between the target lipids and a suitable radical initiator during ESI. Mass-selection of the complex and subsequent laser irradiation give rise to odd-electron ions, which, upon further activation by low-energy CID, result in extensive dissociation of the carbon–carbon bonding framework. RDD is thus able to unambiguously identify double-bond position(s) as well as to differentiate between isomeric branched and non-branched acyl chains within complex lipids. As we will show, however, the non-covalent attachment of radical initiators to lipids is not applicable to the structural analysis of simple lipids such as isomeric fatty acids. Here we describe an alternative strategy tailored to fatty acid analysis that exploits a standard chemical derivatization procedure to covalently attach a chromophore to the lipid that incorporates a UV-labile carbon–iodine bond. Examination of a suite of so-modified fatty acids by both PD and RDD reveals highly sensitive and selective fragmentation that can successfully differentiate isomeric fatty acids differing only in the location of carbon–carbon double bond(s) or branching point(s).

EXPERIMENTAL

Chemicals and reagents

HPLC grade methanol, chloroform, pentane and acetonitrile solvents were obtained from Ajax Finechem (Sydney, NSW, Australia) and were used without further purification. The following fatty acid standards (~99% purity) were purchased

Rapid Communications in Mass Spectrometry

from Nu-Chek Prep (Elysian, MN, USA): linoleic acid FA (9*Z*,12*Z*-18:2); petroselinic acid FA (6*Z*-18:1); petroselaidic acid FA (6*E*-18:1); oleic acid FA (9*Z*-18:1); elaidic acid FA (9*E*-18:1); *cis*-vaccenic acid FA (11*Z*-18:1); ricinoleic acid 12-OHFA (9*Z*-18:1); and 12-hydroxy stearic acid 12-OHFA (18:0). Two saturated (non-branched and branched chains) fatty acid isomers were purchased from Sigma-Aldrich (Castle Hill, Australia): arachidic acid (99%) FA (20:0) and phytanic acid (96%) FA (4Me16:0). Other reagents for derivatization, including boron trifluoride (BF_3) 10% in methanol solution, 4-iodoaniline (98%), 4-iodobenzyl alcohol (97%) and sodium acetate and sulfuric acid (98%), were also purchased from Sigma-Aldrich.

In this manuscript, it is sometimes instructive to indicate the double-bond position within a fatty acid or derivative without specific reference to the stereochemistry. So here we adopt the commonly used Δ^x nomenclature indicating that the double bond is located at the x^{th} carbon–carbon bond counting from the carboxylate moiety,[30] e.g., the carbon–carbon double bond in oleic acid is Δ^9.

Sample preparation

A chemical reaction between a fatty acid and 4-iodobenzyl alcohol is initiated in the presence of a 2% sulfuric acid catalyst (Scheme 1). The esterification procedure was conducted as follows: approximately 1 mg of fatty acid and 5 mg of 4-iodobenzyl alcohol were dissolved in 1 mL acetonitrile in a 3 mL glass vial. Concentrated sulfuric acid (20 μL) was added to the mixture to obtain a final concentration of 2% (v/v) in solution, followed by heating at 80°C for 30–45 min in a water bath. After cooling, water (0.5 mL) and pentane (1 mL) were sequentially added to the solution. The reaction mixture was shaken several times to separate the aqueous and organic components: the desired ester is partitioned into the non-polar organic layer. The upper phase (i.e., pentane) was then collected with a fatty acid 4-iodobenzyl ester (FAIBE) concentration of approximately 3 mM. Prior to ESI-MS experiments, samples were prepared by diluting the pentane extracts to 10–20 μM of fatty acid iodobenzyl derivatives in methanol. Sodium (or lithium) acetate was added to the sample solutions to a final concentration of 50 μM. The FAIBE yields achieved under these conditions were estimated to be >90% with the exception of the hydroxyl fatty acids where yields were ca. 10–50%.

Fatty acid methyl ester derivatives of arachidic acid FA (20:0) and phytanic acid FA (4Me16:0) were prepared by treatment with 10% BF_3 in methanol. The samples used in preparation of non-covalent adducts between FAMEs and 4-iodoaniline were obtained by extracting FAME (20:0) and FAME (4Me16:0) into pentane and diluting this organic layer to a final concentration of 10–20 μM of FAMEs in methanol, then adding 4-iodoaniline 10 μM and 0.2% formic acid.

Instrumentation

All mass spectra were acquired on a modified LTQ linear ion trap mass spectrometer (Thermo Fisher Scientific, San Jose, CA, USA). The sample solutions of fatty acid derivatives were introduced into the ESI source by direct infusion to generate the gaseous sodium adducts. Typical source parameters were: sample flow rate 3 μL min^{-1}, spray voltage +4.5 kV, capillary temperature 250°C, tube lens voltage 129 V, and capillary voltage 49 V. Nitrogen gas served as the sheath (arbitrary flow rate units between 5 and 20), auxiliary and sweep gases (between 0 and 5 arbitrary flow rate units), and helium gas served as the buffer gas. Ions were mass-selected with a window of 1–3 Th and subjected to photodissociation (PD) as described below. Radical-directed dissociation (RDD) mass spectra were acquired by subsequent mass-selection of radical ion photoproducts followed by CID using standard conditions (i.e., manufacturers parameters of *normalized collision energy* and *activation time* are set to 20–25% and 30 ms, respectively). All spectra presented represent an average of 50–100 scans.

The linear ion trap was previously modified[31] to enable PD experiments following the experimental configuration described by Ly and Julian.[32] Briefly, a quartz window (MDC Vacuum Products, Hayward, CA, USA) was installed on the posterior plate of the vacuum housing to allow transmission of 266 nm laser pulses (~30 mJ cm^{-2}) from a flash lamp-pumped Nd:YAG laser (Continuum, Santa Clara, CA, USA). All laser experiments herein were conducted at $\lambda = 266$ nm and the pulse-width of the laser was approximately 5 ns. The laser beam was directed into the trap via two right-angle prisms, which can be adjusted to optimize alignment with the ion cloud. Pulses were synchronized to the beginning of the activation step of a typical MS^n experiment by feeding a TTL pulse from the instrument to the laser via a digital delay generator (Berkeley Nucleonics, San Rafael, CA, USA). Only one laser pulse irradiated the selected ions per mass spectral cycle.

RESULTS AND DISCUSSION

Saturated straight-chain and branched fatty acids

Figure 1 shows photodissociation (PD) mass spectra of protonated 4-iodoaniline (IA) at m/z 220 and of the two non-covalent complexes of this adducting agent with two saturated methyl esters, forming $[FAME\ (20:0) + IA]^+$ and $[FAME\ (4Me16:0) + IA]^+$ precursor ions, both seen at m/z 546.

All three PD spectra in Fig. 1 show only one major product ion at m/z 93 corresponding to an aniline radical cation and, significantly, in the case of the lipid adduct ions, no radical ion incorporating the lipid was observed. The formation,

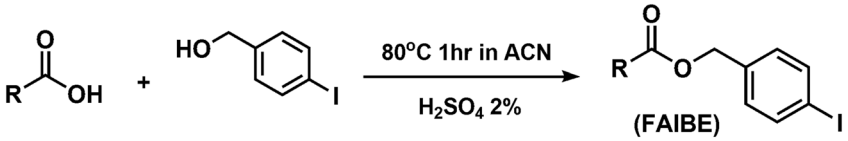

Scheme 1. Derivatization of fatty acids (FAs) to produce fatty acid 4-iodobenzyl esters (FAIBEs).

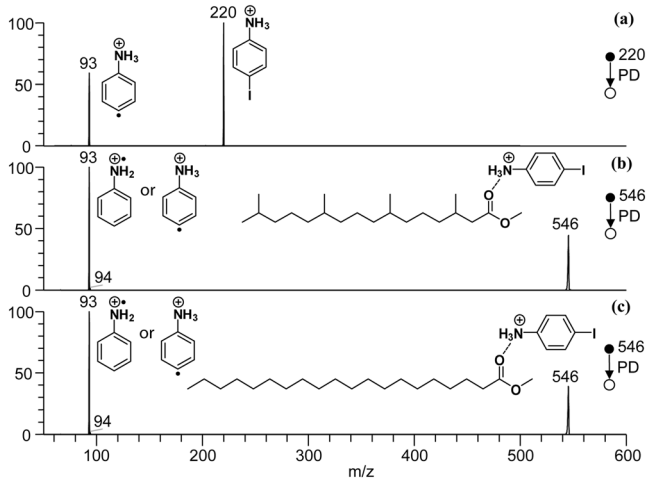

Figure 1. PD mass spectra of (a) protonated 4-iodoaniline, and of non-covalent complexes between protonated 4-iodoaniline with FAMEs of (b) phytanic acid, FAME (4Me16:0) and (c) arachidic acid, FAME (20:0). Structures of the precursor ions are indicated above each spectrum.

and subsequent collisional activation of lipid radical ions derived from PD of such non-covalent complexes, were central to the radical-directed dissociation (RDD) strategy that we have previously employed for complex lipids.[29] The data shown here, however, indicate that, at least in the case of saturated FAMEs, our non-covalent RDD approach is unable to provide any structurally diagnostic fragmentation let alone discriminate between branched and straight-chain fatty acid isomers.

In contrast to the non-covalent complexes described above, the PD mass spectra of covalent 4-iodobenzyl ester derivatives of the same straight-chain and branched fatty acid isomers show rich fragmentation and significant points of differentiation (Figs. 2(a) and 2(c), respectively). These spectra were obtained by isolating the m/z 551 precursor ions for [FAIBE (20:0) + Na]$^+$ and [FAIBE (4Me16:0) + Na]$^+$ and subjecting them to a single laser pulse ($\lambda = 266$ nm). For both isomers the major ionic photoproduct is observed at m/z 424 and corresponds to homolysis of the carbon–iodine bond and formation of a [M + Na − I]$^{\bullet+}$ radical cation. Subsequent mass-selection and CID of this ion in each case gave rise to the RDD mass spectra shown in Figs. 2(b) and 2(d). Similar PD and RDD spectra were obtained for the analogous [M + Li]$^+$ ions (Supplementary Fig. S1, Supporting Information), suggesting that dissociation is predominantly radical-directed rather than charge-directed in these experiments. Proposed radical-directed fragmentation pathways for the branched acyl chain are shown in Scheme 2.

Comparing the PD spectra shown in Figs 2(a) and 2(c) reveals a difference in peak spacing in the low-mass region of the spectra. Specifically, product ions at m/z 172 and 185 ($\Delta m = 13$ Th) are observed for the straight-chain FAIBE (20:0), while ions at m/z 172 and 199 ($\Delta m = 27$ Th) are associated with the methyl-branched chain of FAIBE (4Me16:0). Mechanisms to account for these ions in the latter case are indicated in Scheme 2 (pathways vii and viii). In this proposal, hydrogen atom abstraction by the nascent phenyl radical results in relocation of the radical to the C2 and C4 positions on the fatty acyl chain. Subsequent β-scission from these positions can yield the radical cation at m/z 172 or the closed shell olefin at m/z 199. Applying the same mechanisms to arachidic acid (not shown) yields the identical product ion

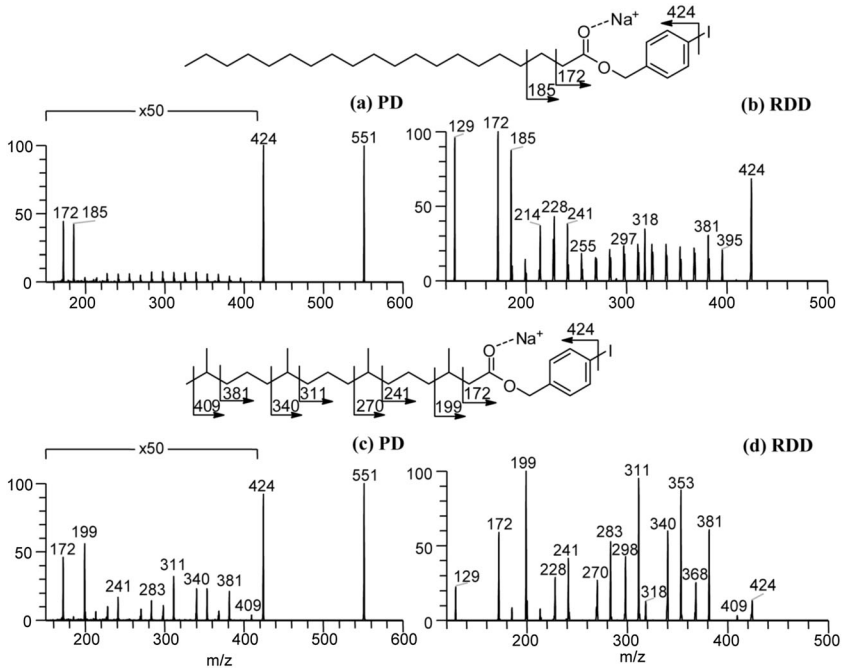

Figure 2. Mass spectra of saturated non-branched vs. branched fatty acid 4-iodobenzyl ester (FAIBE) derivatives. (a, b) PD and RDD mass spectra acquired from arachidic acid, FAIBE (20:0) and (c, d) PD and RDD spectra acquired from phytanic acid FAIBE (4Me16:0).

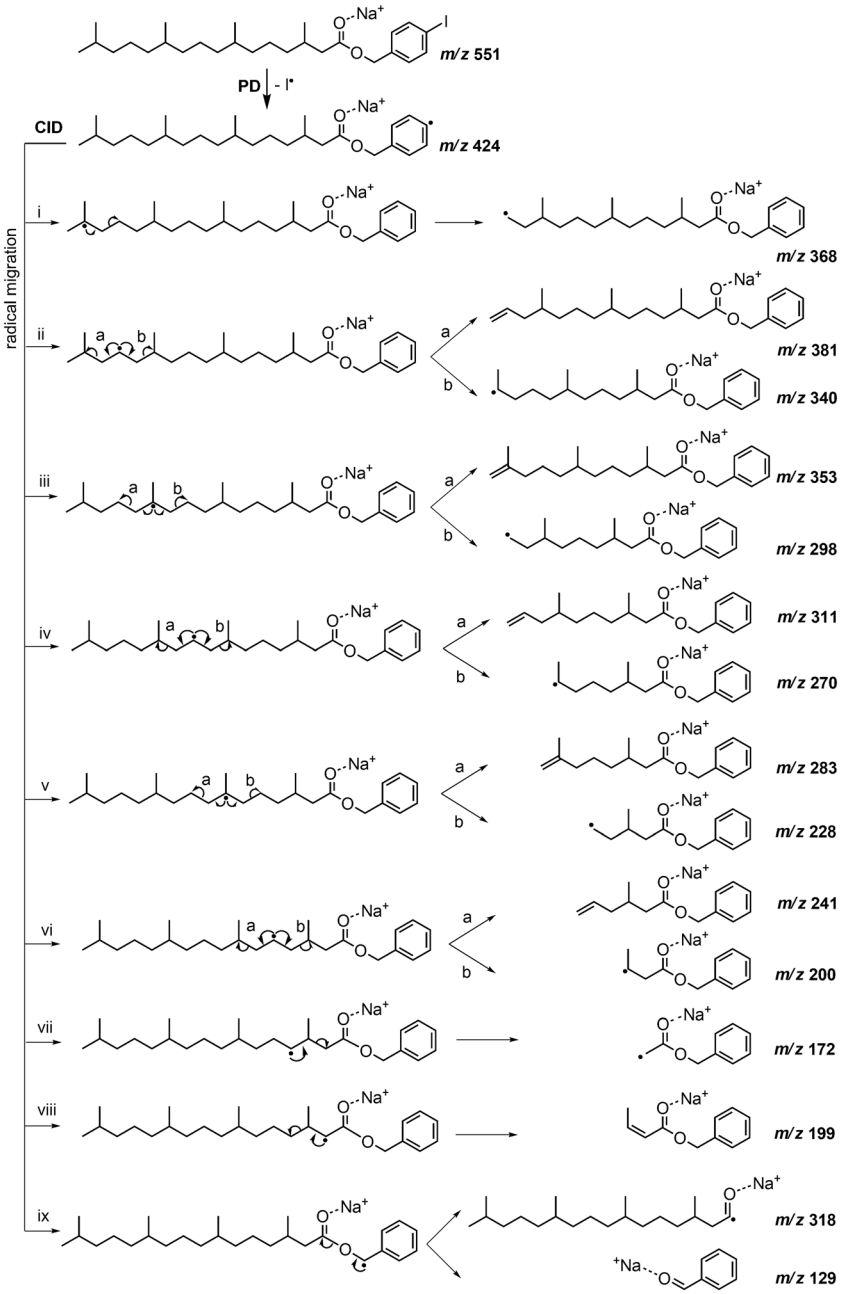

Scheme 2. Proposed fragmentation pathways for FAIBE (4Me16:0) where the m/z values of the product ions correspond to those shown in Fig. 2(d).

at m/z 172 but, in the absence of the C3-methyl branch, β-scission from C2 yields a product ion at m/z 185. These features of the PD spectra alone are sufficient to differentiate the two isomers and further spectral differences are also noted among the lower abundance product ions. These low intensity signals are enhanced by subsequent collisional activation and the resulting RDD spectra are discussed below.

The regular peak spacing observed in the RDD spectrum of the straight-chained arachidic acid in Fig. 2(b) suggest that hydrogen abstraction by the phenyl radical occurs almost uniformly at all methylene positions along the carbon chain. Subsequent β-scission processes from these carbon-centred radicals give rise to a homologous series of radical cations (resulting from neutral alkene elimination) and even-electron olefinic cations (resulting from alkyl radical losses). The superposition of these processes that differ in product ion mass by 1 Th results in the apparent peak doubling observed in Fig. 2(b), for example, m/z 297 and 298 ions result from loss of $C_9H_{19}^{\cdot}$ and alkene C_9H_{18}, respectively. The presence of methyl branching, however, leads to more selective fragmentation patterns in the RDD of FAIBE (4Me16:0) (Fig. 2(d)) where the product ion abundances are found to vary more substantially. The preference for chain cleavage at some positions over others is attributed to the scenarios where either (i) a stabilized tertiary radical located at a branch point undergoes dissociation via β-scission (e.g., Scheme 2 pathway iii) or (ii) dissociation adjacent to a branch point yields a secondary radical product (e.g., Scheme 2 pathway ii).

This rationale is illustrated for all major product ions in Scheme 2 and explains the characteristic alternation between even- and odd-mass product ions observed in Fig. 2(d). It is also noted that the peak spacing observed at each methyl branching point is not always the same. Particularly, $\Delta m = 27$ Th between m/z 199 and 172 is diagnostic for the methyl branch at C3, closest to the carbonyl group (*vide supra*), while $\Delta m = 28$ Th between m/z 409 and 381 is observed for the *iso*-branching point adjacent to the methyl terminus. For other branching points in the middle of the carbon chain, the peak spacing is $\Delta m = 29$ Th at each position (e.g., m/z 340 and 311, and m/z 270 and 241). If found to be consistent in other branched fatty acids, such peak spacings in RDD spectra might prove useful in the differentiation of *iso*- and *anteiso*-branched chain FAs.[18] Importantly, the radical dissociation processes in the RDD spectra of the FAIBE derivatives clearly differentiate straight-chain FA (20:0) from its methyl-branched FA (4Me16:0) isomer (cf. Figs. 2(b) and 2(d)). Moreover, in the latter case, the fragmentation patterns can be used to localize the positions of methyl substituents.

Monounsaturated fatty acids

Three isomeric monounsaturated fatty acids, namely FA (11Z-18:1), FA (9Z-18:1) and FA (6Z-18:1), were derivatized as 4-iodobenzyl esters and subjected to ESI in the presence of sodium acetate. The resulting $[M + Na]^+$ ions were then irradiated by a single laser pulse ($\lambda = 266$ nm) and the resulting PD mass spectra are shown in Fig. 3. While in all three instances

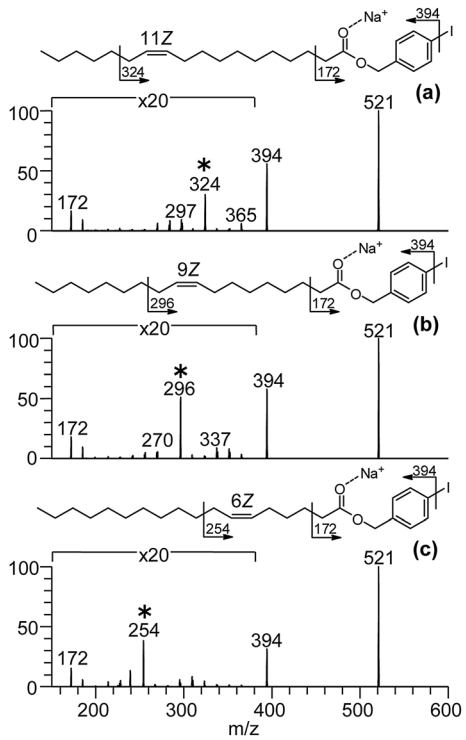

Figure 3. Photodissociation (PD) mass spectra acquired from monounsaturated isomers $[FAIBE\ (18:1) + Na]^+$ derivatized from (a) FA (11Z-18:1), (b) FA (9Z-18:1), and (c) FA (6Z-18:1). The symbol * indicates the diagnostic product ion formed selectively from each double bond positional isomer.

the most abundant product ions are assigned as the loss of atomic iodine (i.e., $[M + Na - I]^{\bullet +}$ at m/z 394) the next most abundant product ions are distinct in each case (i.e., m/z 324, 296 and 254 in Figs. 3(a)–3(c), respectively). Although some magnification is required to visualize these product ions, the PD spectra display excellent signal-to-noise and thus these diagnostic signals can readily be used to differentiate between the three isomers. Furthermore, the neutral losses of the radicals $C_5H_{11}^{\bullet}$, $C_7H_{15}^{\bullet}$ and $C_{10}H_{21}^{\bullet}$ in the spectra shown in Figs. 3(a)–3(c), respectively, are consistent with homolytic cleavage of the allylic carbon–carbon bond implicating a common mechanism in each case.

Energetically, the initial phenyl radical formed following photolysis of the carbon–iodine bond can abstract any hydrogen atom from the carbon chain due to the higher carbon–hydrogen bond dissociation energy of benzene (~113 kcal mol^{-1}) than the aliphatic carbon–hydrogen bond energies (~96 kcal mol^{-1}).[33] As a result, facile hydrogen atom transfer from a range of sites on the fatty acyl chain is expected and several representative structures resulting from this initial rearrangement are indicated in Scheme 3. In some instances the radical will be at a stabilized position such as the α-position (adjacent to the carbonyl moiety) or the allylic positions (adjacent to the carbon-carbon double bond), examples of which are indicated in Schemes 3(b) and 3(d), respectively. Even in instances where the radical does not transfer directly to these positions, subsequent hydrogen atom transfer events will also be thermodynamically favorable leading to an eventual cascade to stabilized positions. Indeed, Ly and Julian have estimated that in RDD of peptides and proteins up to three such sequential hydrogen atom transfers may occur until the radical becomes localized at energetically favored positions.[34] As a consequence of these processes, the bulk of the ion population that survives the initial photolysis event is expected to be made up of stabilized radical cations and it is these species which will be isolated for subsequent CID in RDD experiments (see later). In contrast, if the initial hydrogen atom abstraction occurs adjacent to an activated bond, direct *β*-scission results. Two such examples are illustrated for FAIBE (9Z-18:1) in Schemes 3(a) and 3(c) and correspond to the formation of the resonance-stabilized ester enolate (m/z 172) and allyl (m/z 296) radical cations, respectively. The selectivity of the latter pathway makes this a particularly useful diagnostic for double-bond position and thus provides an alternative means of selective identification and differentiation of unsaturated fatty acids.

Subsequent CID performed on the abundant radical ions at m/z 394 from each of the monounsaturated FAIBE isomers gave rise to rich RDD fragmentation, as illustrated in Fig. 4. At a glance, the base peaks observed in all three RDD spectra are distinct (i.e., m/z 337, 309 and 239 in Figs. 4(a)–4(c), respectively) thus representing a characteristic ion for each isomer. In Fig. 4(a), the base peak at m/z 337 corresponds to a neutral loss of a $C_4H_9^{\bullet}$ radical (57 Da), which probably involves *β*-scission from an allyl radical adjacent to the Δ^{11} double bond (Scheme 4(a)). By extension of this mechanism, when the position of unsaturation is at Δ^9, as for FAIBE (9Z-18:1), a 28 Th shift of the most abundant RDD product ion is predicted. This corresponds to a $C_6H_{13}^{\bullet}$ loss (Scheme 4(b)), and indeed the ion produced *via* this mechanism is observed at m/z 309 in Fig. 4(b). Similarly, the same process occurring in FAIBE (6Z-18:1) would give rise to a product ion at m/z 267 from loss of a $C_9H_{19}^{\bullet}$ radical. While this ion is

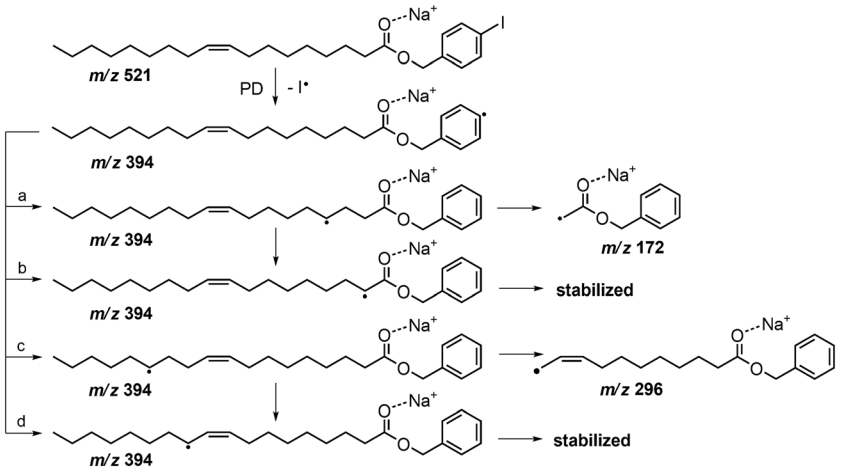

Scheme 3. Proposed mechanism for radical rearrangement and dissociation resulting from PD of 4-iodobenzyl ester derivative of oleic acid. Note that only representative examples of isomerization and/or dissociation pathways of the radical cation are shown.

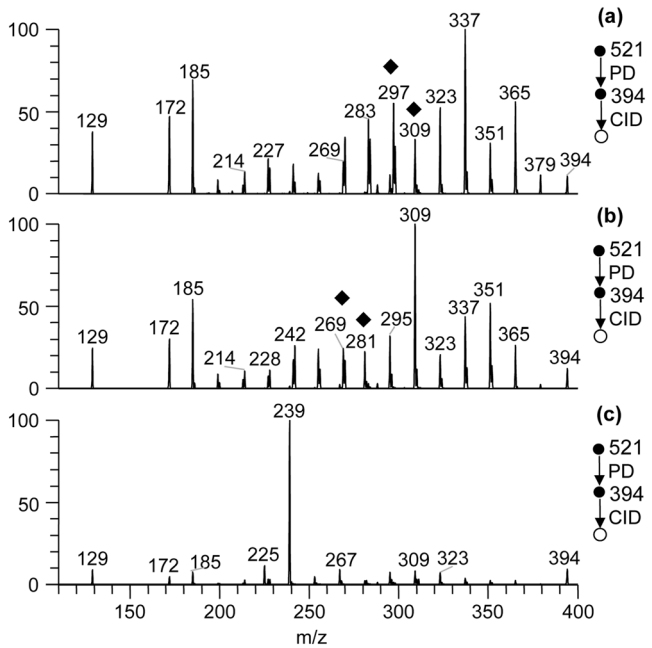

Figure 4. RDD spectra resulting from the PD-generated $[M + Na - I]^{\bullet +}$ radical cation m/z 394 from 4-iodobenzyl ester derivatives: (a) FAIBE (11Z-18:1); (b) FAIBE (9Z-18:1); and (c) FAIBE (6Z-18:1). Product ions with a spacing of 12 Th indicative of carbon–carbon double-bond position are labelled with ◆ symbols.

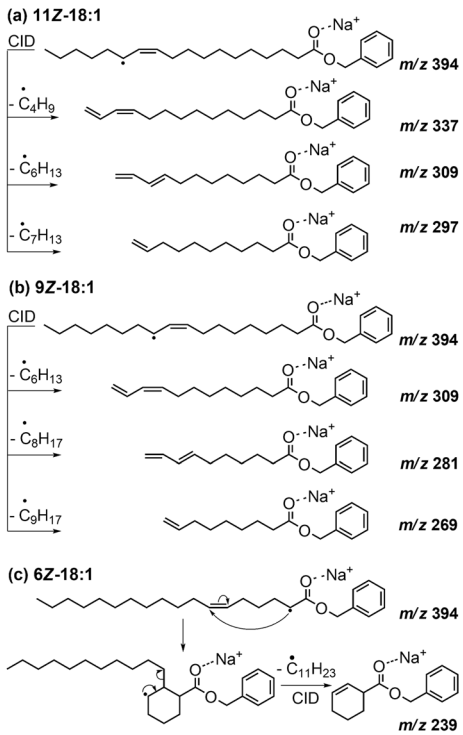

Scheme 4. Proposed mechanism of RDD fragmentation observed from (a) FAIBE (11Z-18:1); (b) FAIBE (9Z-18:1); and (c) FAIBE (6Z-18:1).

observed in the RDD spectrum, it is of low abundance and the spectrum shown in Fig. 4(c) is instead dominated by the product ion at m/z 239 suggesting that a competing pathway exists for this isomer that results in loss of a $C_{11}H_{23}$ radical. One possible explanation for the preferential formation of the m/z 239 signal for this isomer is the process outlined in Scheme 4(c). In this mechanism, activation of the stabilized ester enolate radical results in cyclization and addition to the Δ^6-double bond to form a six-membered ring. Subsequent β-scission from this intermediate could give rise to the observed $C_{11}H_{23}^{\bullet}$ radical loss. The formation of a six-membered ring for FAIBE (6Z-18:1) is expected to be favorable, while the same process will become disfavored for double-bond positions beyond Δ^6 due to entropic constraints.

In contrast to the formation of a single dominant product ion, as observed for FAIBE (6Z-18:1) (Fig. 4(c)), the RDD spectra of FAIBE (9Z-18:1) and FAIBE (11Z-18:1) isomers (Figs. 4(a) and 4(c)) reveal extensive fragmentation of the hydrocarbon chain. The product ions observed correspond to dissociation arising from almost all positions suggesting that dissociation

is preceded by radical migration. By analogy to saturated fatty acids discussed earlier (cf. Scheme 2), these product ions can be rationalized as resulting from a series of alkyl radical or alkene losses. The regular peak spacing of 14 Th that arises from these processes is interrupted by the carbon–carbon double bond providing a distinctive 12 Th spacing as indicated by the symbols ♦ in Fig. 4, e.g., *m/z* 309 and 297 in Fig. 4(a). The characteristic 12 Th peak spacing suggests that RDD spectra of FAIBE derivatives could be used to locate position(s) of unsaturation within unknown lipids. Interestingly, this peak spacing pattern is consistent with that reported for unsaturated fatty acid derivatives upon EI[12,13] and high-energy CID.[35,36]

The sensitivity of both PD and RDD processes to the configuration of the carbon–carbon double bond was also investigated. FAIBE derivatives of the elaidic acid FA (9*E*-18:1) and petroselaidic FA (6*E*-18:1) acids were prepared, both of which have *trans* stereochemistry about their double bonds. The PD and RDD spectra obtained from the sodium adduct ions of these derivatives are provided as Supplementary Figs. S2 and S3, respectively (see Supporting Information), and are indistinguishable from those acquired from their *cis* counterparts, oleic and petroselinic, shown in Figs. 3 and 4. While the inability to differentiate stereoisomers by this approach was disappointing it was not altogether unexpected given that the thermodynamic preference for hydrogen atom abstraction from the allylic position(s) in unsaturated lipids is largely independent of stereochemistry. Indeed, the formation of allylic radicals such as those indicated in Schemes 3 and 4 results in a loss of stereochemical information.

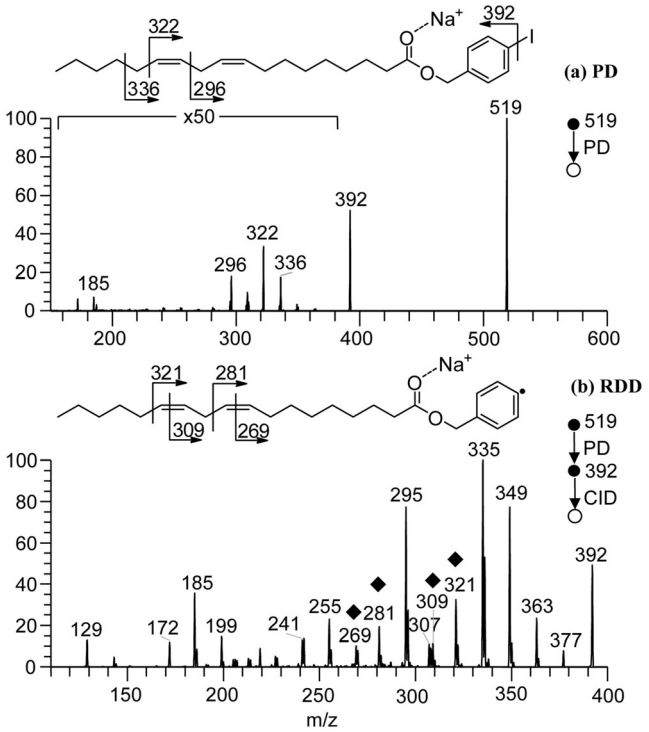

Figure 5. (a) The PD spectrum of the $[M + Na]^+$ ion of FAIBE (9*Z*,12*Z*-18:2) linoleic acid. (b) The RDD spectrum acquired by collisional activation of the *m/z* 392 radical ion formed in (a). Adjacent peaks with 12 Th spacing indicated in the position of carbon–-carbon double bonds are labelled with ♦ symbols.

Polyunsaturated fatty acid

In order to investigate the photo-fragmentation behavior of polyunsaturated fatty acids, 4-iodobenzyl ester derivatives of linoleic acid were prepared and subjected to both PD and RDD (Figs. 5(a) and 5(b), respectively). PD of the mass-selected $[M + Na]^+$ ion of FAIBE (9*Z*,12*Z*-18:2) at *m/z* 519 gives rise to predominantly the $[M + Na - I]^{\bullet +}$ ion at *m/z* 392 (Fig. 5(a)). Several lower abundance photo-fragments are also observed in this spectrum. The product ions at *m/z* 336 and 296 correspond to neutral loss of atomic iodine followed by losses of the C_4H_8 and C_7H_{12} alkenes, respectively. By analogy with the mono-unsaturated systems discussed above, these ions can be rationalized as resulting from dissociation of activated carbon–carbon bonds and formation of a radical cation incorporating the stabilized allyl radical moiety (cf. Scheme 3(c)). In contrast, the product ion at *m/z* 322, corresponding to the neutral loss of a C_5H_{10} alkene with cleavage at the vinylic position, appears to be characteristic of the homoallylic diene motif. The RDD spectrum shown in Fig. 5(b) was acquired from CID of the PD-generated radical ions at *m/z* 392. The fragmentation pattern of the polyunsaturated fatty acid is clearly distinguishable from those of the mono-unsaturates previously discussed. Notably, the product ion spacing of 12 Th (labelled with ♦ in Fig. 5(b)) is repeated twice in the RDD spectrum of the linoleic acid derivative. The first of these is noted between *m/z* 321 and 309, corresponding to $C_5H_{11}^{\cdot}$ and $C_6H_{11}^{\cdot}$ neutral alkyl and alkenyl radical losses resulting from vinylic and allylic carbon–carbon bond cleavages and indicative of the Δ^{12} double bond. Similarly, the second distinctive ion pair observed at *m/z* 281 and 269 coincides with the location of the second Δ^9-double bond. An interesting 'double peak' feature is also observed in Fig. 5(b) with abundant ions at both *m/z* 309 and 307, suggestive of competing pathways for cleavage at the Δ^{12}-double bond that result in neutral losses of unsaturated ($C_6H_{11}^{\cdot}$) and saturated radicals ($C_6H_{13}^{\cdot}$), respectively. The approximately equal abundance of these two product ions appears to be a characteristic feature of the 18:2 acyl chain as the equivalent ions are of low or negligible abundance for both the mono-unsaturated 18:1 analogues (e.g., note the low abundance of *m/z* 295 relative to *m/z* 297 in Fig. 4(a)) and indeed, the equivalent C9 losses from 18:2 (i.e., no *m/z* 267 partners the *m/z* 269 in Fig. 5(b)) While the mechanistic origins of this 'double peak' remain to be demonstrated, there is some analogy to our prior observations in the RDD spectra of complex lipids.[29] Overall, these data confirm that the key structural features of the polyunsaturated fatty acid are retained in the radical ion formed upon photodissociation of the 4-iodobenzyl ester derivative. Moreover, the subsequent dissociation of this species gives rise to a fragmentation pattern from which the initial structure can be gleaned.

Hydroxy fatty acids

Hydroxy fatty acids (OHFA) are an abundant lipid class found in foodstuffs,[37,38] along with bacteria and fungi.[39,40] The specific location of hydroxylation is reported to affect metabolic functionality,[41,42] necessitating analytical methods capable of elucidating the location of such motifs. Shown in Fig. 6(a) is a PD spectrum generated following photolysis of mass-selected $[M + Na]^+$ ions (at *m/z* 539) of the 4-iodobenzyl ester derivative of 12-hydroxystearic acid. The most

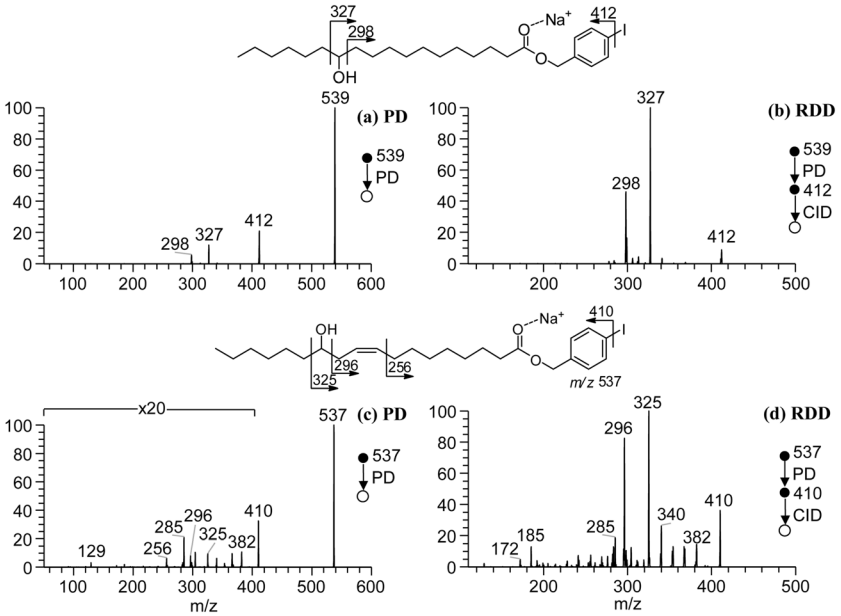

Figure 6. Mass spectra acquired from 4-iodobenzyl ester derivatives of the hydroxy fatty acids 12-OHFA (18:0) and 12-OHFA (9Z-18:1). (a) The PD spectrum of the $[M+Na]^+$ adduct ion of the 12-OHFA (18:0) derivative at m/z 539 and (b) the RDD spectrum acquired by performing subsequent CID on the m/z 412 radical ion. (c) The PD spectrum of the $[M+Na]^+$ adduct ion of the 12-OHFA (9Z-18:1) derivative at m/z 537 and (d) the RDD spectrum acquired by performing subsequent CID on the m/z 410 radical ion.

abundant product ion in this spectrum is observed at m/z 412 and corresponds to the radical cation formed upon loss of atomic iodine. Subsequent CID of this species yields the RDD spectrum shown in Fig. 6(b). Two major product ions can be seen in both PD and RDD spectra and represent the losses of $C_7H_{14}O$ (m/z 298) and $C_6H_{13}^{\bullet}$ (m/z 327) from the $[M+Na-I]^{\bullet+}$ radical cation. Both product channels could derive from β-scission reactions directed from an alkoxyl radical at the 12-position, as indicated in Scheme 5. The dominance of these product ions over those arising from carbon-centred radicals points to a preference for hydrogen abstraction from the hydroxyl moiety. Simple enthalpic arguments do not account for this selectivity, however, with the oxygen–hydrogen bond dissociation energies of alcohols typically higher (~105 kcal mol^{-1}) than those of carbon–hydrogen bonds (~96 kcal mol^{-1}).[33] Rather we propose that this selectivity might arise from the proximity of the hydroxyl group to the phenyl-iodide moiety in the three-dimensional structure of the gas-phase ion. It seems plausible that in such a structure the hydroxyl group, along with the ester oxygens, would interact directly with the sodium cation, placing the former in the vicinity of the benzyl ester moiety and thus the nascent phenyl radical upon liberation by photolysis.

For comparison, the unsaturated hydroxyl fatty acid 12-OHFA (9Z-18:1) – a major component of castor oil[43] – was also investigated. PD and RDD mass spectra obtained from the 4-iodobenzyl ester derivatives are shown in Figs. 6(c) and 6(d), respectively. While the PD spectrum is more complex than that of the corresponding saturated analogue (cf. Figs. 6(a) and 6(c)), ions indicative of the location of the hydroxyl moiety and the double bond are clearly

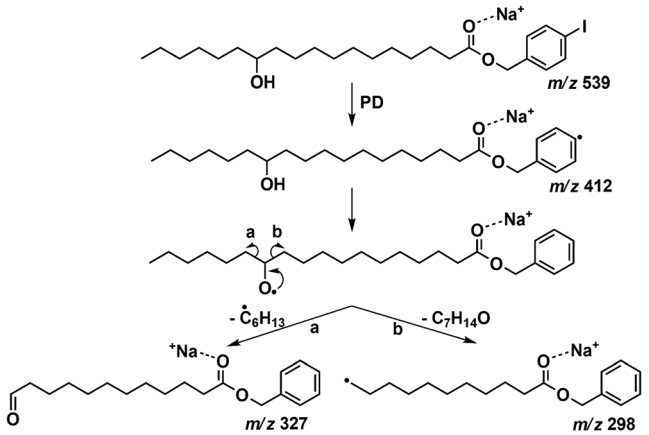

Scheme 5. A proposed dissociation mechanism to account for the formation of major product ions at m/z 298 and 327 resulting from decomposition of the radical cation at m/z 412 generated by PD of the 4-iodobenzyl ester derivative of 12-OHFA (18:0).

observed at m/z 296 ($-C_7H_{14}O$) and 325 ($-C_6H_{13}^{\bullet}$). Indeed the RDD spectrum, obtained by subsequent CID on the $[M+Na-I]^{\bullet+}$ ion at m/z 410, is dominated by these two product ions. In summary, both OHFA investigated here show abundant free radical-driven dissociation at the site of the hydroxyl moiety. These findings suggest that either PD or RDD could be deployed to describe the site(s) of hydroxylation in an unknown OHFA.

CONCLUSIONS

The standard esterification procedure employed here to produce the required FAIBE derivatives was successfully demonstrated for a variety of structurally diverse fatty acids. In general, the esterification was high-yielding with the exception of the hydroxy fatty acids for which competing reactions (probably intramolecular lactonization) reduced the efficiency of the desired conversion. Nonetheless, even in this case, sufficient FAIBE was formed to demonstrate the effectiveness of the photodissociation strategy and alternative esterification protocols could be employed to improve this yield if required. Ionization of the FAIBE derivatives as sodium adducts and subsequent laser-photolysis at 266 nm was found to be efficient in the generation of the desired radical ions with yields of between 30 and 100% of the precursor ion abundance. In addition to the expected iodine loss, several of the derivatized fatty acids showed distinct fragmentation patterns upon photolysis. In particular, cleavage of activated carbon–carbon bonds was observed, such as homolysis of allylic carbon–carbon bonds in unsaturated fatty acids. This selective fragmentation upon photoactivation might find application in selective screening of complex lipid mixtures for specific motifs such as double-bond position(s) or sites of hydroxylation. For example, undertaking PD on a mass spectrometer of triple quadrupole geometry (such as that recently described by Dugourd, Lemoine and their co-workers[44]) would allow multiple reaction monitoring or neutral loss scans to be undertaken targeting a particular structural motif or individual fatty acid isomer present within a complex mixture.

Subsequent CID of the $[M + Na - I]^{\bullet +}$ radical cations formed from these FAIBE derivatives gives rise to rich, radical-driven fragmentation and the resulting RDD mass spectra made it possible to distinguish between isomeric fatty acids. The usual mass difference between peaks is representative of the succession of methylene groups of the carbon chain. Thus, RDD of derivatized fatty acids containing saturated, non-branched acyl chains are characterized by spectra with regular peak spacings of 14 Th between successive neutral losses in the alkyl radical or alkene series. In the same way, any increase in the spacings between adjacent groups of peaks provides evidence for the presence of branching features or even hydroxylation in the acyl chain. For example, spacings of 27/28/29 Th were shown to locate both (i) the positions of the methyl-branched chain for the phytanic acid derivative (cf. Fig. 2d) and (ii) the position of hydroxylation in 12-hydroxystearic acid (cf. Fig. 6(b)). Similarly, a decrease in peak spacing to 12 Th was observed to arise at the position(s) of carbon–carbon double bonds within unsaturated fatty acids.

In conclusion, we have presented here a novel approach to lipid structure elucidation that is particularly suited to describing simple lipids such as fatty acids. The requirement to incorporate a chromophore and a photolabile moiety was readily satisfied in this instance by incorporation of 4-iodobenzyl alcohol by standard esterification procedures. As noted in the introduction however, a wide range of fatty acid derivatization procedures have previously been described (e.g., DMOX derivatives) and many of these could be readily adapted to satisfy the requirements of RDD. It is thus attractive to consider exploitation of alternative derivatives that may allow for improved derivatization and/or ionization efficiencies and even greater selectivity in radical-directed fragmentation.

SUPPORTING INFORMATION

Additional supporting information may be found in the online version of this article.

Acknowledgements

S.J.B., A.J.T. and T.W.M. are grateful to the Australian Research Council (DP0986628 and DP120102922) and the University of Wollongong for funding. H.T.P. was supported by a matching scholarship from the University of Wollongong, T.W.M. is an Australian Research Council *Future Fellow* (FT110100249) and S.J.B. and A.J.T are supported by the Australian Research Council's Centre of Excellence for Free Radical Chemistry and Biotechnology (CE0561607).

REFERENCES

[1] G. Dobson, W. W. Christie. Mass spectrometry of fatty acid derivatives. *Eur. J. Lipid Sci. Technol.* **2002**, *104*, 36.
[2] C. K. Van Pelt, J. T. Brenna. Acetonitrile chemical ionization tandem mass spectrometry to locate double bonds in polyunsaturated fatty acid methyl esters. *Anal. Chem.* **1999**, *71*, 1981.
[3] J. F. Rontani, N. Zabeti, C. Aubert. Double bond migration to methylidene positions during electron ionization mass spectrometry of branched monounsaturated fatty acid derivatives. *J. Am. Soc. Mass Spectrom.* **2009**, *20*, 1997.
[4] L. Hejazi, D. Ebrahimi, M. Guilhaus, D. B. Hibbert. Discrimination among geometrical isomers of α-linolenic acid methyl ester using low energy electron ionization mass spectrometry. *J. Am. Soc. Mass Spectrom.* **2009**, *20*, 1272.
[5] J. K. G. Kramer, C. Cruz-Hernandez, J. Zhou. Conjugated linoleic acids and octadecenoic acids: Analysis by GC. *Eur. J. Lipid Sci. Technol.* **2001**, *103*, 600.
[6] M. Petrović, N. Kezić, V. Bolanča. Optimization of the GC method for routine analysis of the fatty acid profile in several food samples. *Food Chem.* **2010**, *122*, 285.
[7] H. Martinez-Seara, T. Róg, M. Pasenkiewicz-Gierula, I. Vattulainen, M. Karttunen, R. Reigada. Interplay of unsaturated phospholipids and cholesterol in membranes: effect of the double-bond position. *Biophys. J.* **2008**, *95*, 3295.
[8] S. H. J. Brown, T. W. Mitchell, S. J. Blanksby. Analysis of unsaturated lipids by ozone-induced dissociation. *Biochim. Biophys. Acta* **2011**, *1811*, 807.
[9] T. W. Mitchell, H. T. Pham, M. C. Thomas, S. J. Blanksby. Identification of double bond position in lipids: From GC to OzID. *J. Chromatogr. B* **2009**, *877*, 2722.
[10] D. J. Harvey. Picolinyl esters for the structural determination of fatty acids by GC/MS. *Mol. Biotechnol.* **1998**, *10*, 251.
[11] W. W. Christie. Gas chromatography-mass spectrometry methods for structural analysis of fatty acids. *Lipids* **1998**, *33*, 343.
[12] J. T. G. Hamilton, W. W. Christie. Mechanisms for ion formation during the electron impact-mass spectrometry of picolinyl ester and 4,4-dimethyloxazoline derivatives of fatty acids. *Chem. Phys. Lipids* **2000**, *105*, 93.
[13] G. Dobson, W. W. Christie. Structural analysis of fatty acids by mass spectrometry of picolinyl esters and dimethyloxazoline derivatives. *Trends Anal. Chem.* **1996**, *15*, 130.

[14] R. R. Ran-Ressler, D. Sim, A. M. O'Donnell-Megaro, D. E. Bauman, D. M. Barbano, J. T. Brenna. Branched chain fatty acid content of United States retail cow's milk and implications for dietary intake. *Lipids* **2011**, *46*, 569.
[15] A. Adida, F. Spener. Intracellular lipid binding proteins and nuclear receptors involved in branched-chain fatty acid signaling. *Prostaglandins, Leukotrienes Essent. Fatty Acids* **2002**, *67*, 91.
[16] M. Kniazeva, Q. T. Crawford, M. Seiber, C.-Y. Wang, M. Han. Monomethyl branched-chain fatty acids play an essential role in *Caenorhabditis elegans* development. *PLoS Biol.* **2004**, *2*, e257.
[17] J. A. Zirrolli, R. C. Murphy. Low-energy tandem mass spectrometry of the molecular ion derived from fatty acid methyl esters: a novel method for analysis of branched-chain fatty acids. *J. Am. Soc. Mass Spectrom.* **1993**, *4*, 223.
[18] R. R. Ran-Ressler, P. Lawrence, J. T. Brenna. Structural characterization of saturated branched chain fatty acid methyl esters by collisional dissociation of molecular ions generated by electron ionization. *J. Lipid Res.* **2012**, *53*, 195.
[19] M. P. Yurawecz, K. M. Morehouse. Silver-ion HPLC of conjugated linoleic acid isomers. *Eur. J. Lipid Sci. Technol.* **2001**, *103*, 609.
[20] U. Sommer, H. Herscovitz, F. K. Welty, C. E. Costello. LC-MS-based method for the qualitative and quantitative analysis of complex lipid mixtures. *J. Lipid Res.* **2006**, *47*, 804.
[21] B. Damyanova, S. Momtchilova, S. Bakalova, H. Zuilhof, W. W. Christie, J. Kaneti. Computational probes into the conceptual basis of silver ion chromatography: I. Silver(I) ion complexes of unsaturated fatty acids and esters. *J. Mol. Struc-Theochem* **2002**, *589/590*, 239.
[22] B. N. Damyanova. Retention of lipids in silver ion high-performance liquid chromatography: Facts and assumptions. *J. Chromatogr. A* **2009**, *1216*, 1815.
[23] K. Yang, Z. Zhao, R. W. Gross, X. Han. Identification and quantitation of unsaturated fatty acid isomers by electrospray ionization tandem mass spectrometry: A shotgun lipidomics approach. *Anal. Chem.* **2011**, *83*, 4243.
[24] F.-F. Hsu, J. Turk. Elucidation of the double-bond position of long-chain unsaturated fatty acids by multiple-stage linear ion-trap mass spectrometry with electrospray ionization. *J. Am. Soc. Mass Spectrom.* **2008**, *19*, 1673.
[25] M. C. Thomas, S. R. Dunn, J. Altvater, S. G. Dove, G. W. Nette. Rapid identification of long-chain polyunsaturated fatty acids in a marine extract by HPLC-MS using data-dependent acquisition. *Anal. Chem.* **2012**, *84*, 5976.
[26] S. R. Ellis, J. R. Hughes, T. W. Mitchell, M. i. h. Panhuis, S. J. Blanksby. Using ambient ozone for assignment of double bond position in unsaturated lipids. *Analyst* **2012**, *137*, 1100.
[27] M. K. Moe, T. Anderssen, M. B. Strom, E. Jensen. Total structure characterization of unsaturated acidic phospholipids provided by vicinal di-hydroxylation of fatty acid double bonds and negative electrospray ionization mass spectrometry. *J. Am. Soc. Mass Spectrom.* **2005**, *16*, 46.
[28] M. C. Thomas, T. W. Mitchell, D. G. Harman, J. M. Deeley, J. R. Nealon, S. J. Blanksby. Ozone-induced dissociation: Elucidation of double bond position within mass-selected lipid ions. *Anal. Chem.* **2008**, *80*, 303.
[29] H. T. Pham, T. Ly, A. J. Trevitt, T. W. Mitchell, S. J. Blanksby. Differentiation of complex lipid isomers by radical-directed dissociation mass spectrometry. *Anal. Chem.* **2012**, *84*, 7525.
[30] UPAC-IUB Commission on Biochemical Nomenclature. The nomenclature of lipids. *Eur. J. Biochem.* **1977**, *79*.
[31] T. Ly, B. B. Kirk, P. I. Hettiarachchi, B. L. J. Poad, A. J. Trevitt, G. da Silva, S. J. Blanksby. Reactions of simple and peptidic alpha-carboxylate radical anions with dioxygen in the gas phase. *Phys. Chem. Chem. Phys.* **2011**, *13*, 16314.
[32] T. Ly, R. R. Julian. Residue-specific radical-directed dissociation of whole proteins in the gas phase. *J. Am. Chem. Soc.* **2008**, *130*, 351.
[33] S. J. Blanksby, G. B. Ellison. Bond dissociation energies of organic molecules. *Acc. Chem. Res.* **2003**, *36*, 255.
[34] T. Ly, R. R. Julian. Elucidating the tertiary structure of protein ions in vacuo with site specific photoinitiated radical reactions. *J. Am. Chem. Soc.* **2010**, *132*, 8602.
[35] W. J. Griffiths, Y. Yang, J. Å. Lindgren, J. Sjövall. Charge remote fragmentation of fatty acid anions in 400 eV collisions with xenon atoms. *Rapid Commun. Mass Spectrom.* **1996**, *10*, 21.
[36] W. J. Griffiths. Tandem mass spectrometry in the study of fatty acids, bile acids, and steroids. *Mass Spectrom. Rev.* **2003**, *22*, 81.
[37] G. Knothe, S. C. Cermak, R. L. Evangelista. Methyl esters from vegetable oils with hydroxy fatty acids: Comparison of lesquerella and castor methyl esters. *Fuel* **2012**, *96*, 535.
[38] R. Jenske, W. Vetter. Concentrations of medium-chain 2- and 3-hydroxy fatty acids in foodstuffs. *Food Chem.* **2009**, *114*, 1122.
[39] J. H. Skerratt, P. D. Nichols, J. P. Bowman, L. I. Sly. Occurrence and significance of long-chain (ω-1)-hydroxy fatty acids in methane-utilizing bacteria. *Org. Geochem.* **1992**, *18*, 189.
[40] V. M. Dembitsky, T. Rezanka, E. E. Shubinat. Unusual hydroxy fatty acids from some higher fungi. *Phytochemistry* **1993**, *34*, 1057.
[41] R. Ferrando, B. Szponar, A. Sánchez, L. Larsson, P. L. Valero-Guillén. 3-Hydroxy fatty acids in saliva as diagnostic markers in chronic periodontitis. *J. Microbiol. Methods* **2005**, *62*, 285.
[42] A. M. Tonin, M. Grings, E. N. B. Busanello, A. P. Moura, G. C. Ferreira, C. M. Viegas, C. G. Fernandes, P. F. Schuck, M. Wajner. Long-chain 3-hydroxy fatty acids accumulating in LCHAD and MTP deficiencies induce oxidative stress in rat brain. *Neurochem. Int.* **2010**, *56*, 930.
[43] A. T. James, H. C. Hadaway, J. P. W. Webb. The biosynthesis of ricinoleic acid. *Biochem. J.* **1965**, *95*, 448.
[44] Q. Enjalbert, R. Simon, A. Salvador, R. Antoine, S. Redon, M. M. Ayhan, F. Darbour, S. Chambert, Y. Bretonnière, P. Dugourd, J. Lemoine. Photo-SRM: laser-induced dissociation improves detection selectivity of selected reaction monitoring mode. *Rapid Commun. Mass Spectrom.* **2011**, *25*, 3375.

